TRNSYS Dynamic Simulation Model of a Typical Air-Handling Unit: Experimental Calibration and Validation Based on Field Operation Data in the South of Italy

Antonio Rosato – University of Campania Luigi Vanvitelli, Italy – antonio.rosato@unicampania.it
Rita Mercuri – University of Campania Luigi Vanvitelli, Italy – rita.mercuri@unicampania.it
Mohammad El Youssef – University of Campania Luigi Vanvitelli, Italy – mohammad.elyoussef@unicampania.it
Francesco Romanucci – University of Campania Luigi Vanvitelli, Italy – francesco.romanucci1@studenti.unicampania.it
Mohamed G. Ghorab – Alexandria University, Egypt – Mohamed.Ghorab@Alexu.edu.eg

Abstract

The building sector is responsible for about 36% of global final energy use and Heating, Ventilation and Air-Conditioning (HVAC) systems are responsible for about 50÷60% of the building sector's energy demand. In this paper, a detailed dynamic simulation model of a typical HVAC system including a single duct dual-fan constant air volume Air-Handling Unit (AHU) has been developed via the TRaNsient SYStems software platform (TRNSYS 18). The simulation outputs were compared with field operation data measured during 14 experiments performed with reference to a fully instrumented HVAC set-up serving the SENS i-Lab of the Department of Architecture and Industrial Design of the University of Campania Luigi Vanvitelli (Aversa, south of Italy). The comparison was carried out to validate and assess the simulation model accuracy. The results highlighted a high capability of the developed model in simulating the experimental behaviour, with maximum percentage differences between the predicted and experimental values up to -6.0%, 18.3%, -9.1%, -10.6%, -15.3% in terms of heating coil energy, cooling coil energy, humidifier electric demand, heat pump electric consumption and refrigerating system electricity request, respectively.

1. Introduction

1.1 Background

The building sector is a major contributor to climate change, accountable for over 36% of the world's total energy consumption and roughly 37% of its greenhouse gas emissions (Global Status Report, 2022). Heating, Ventilation and Air-Conditioning (HVAC) systems are the most used equipment for maintaining indoor comfort in buildings. The most common HVAC systems include Air-Handling Units (AHUs) that are made up of a number of sensors and parts (such as fans, coils, valves, dampers, filters, actuators, etc.). HVAC systems represent a significant source of energy consumption together with a significant environmental impact; in particular, they are responsible for about 50÷60% of the building sector's energy demand and 10÷20% of the overall energy consumption (Cao et al., 2016; Mirnaghi et al., 2020). Therefore, optimizing the design and performance of such systems can be an important solution to reduce the relative consumption and environmental impact. These challenges can be addressed from an experimental or numerical point of view; taking into account the significant time and resources that are required for field study and lab research (Granderson et al., 2020; Mitali et al., 2021), utilization of accurate simulation models for HVAC systems emerges as a promising alternative option, offering several potential advantages, such as: a) conducting sensitivity and what-if analyses in order to better understand the performance upon varying the boundary conditions, b) suggesting innovative solutions and optimization actions to enhance energy performance, greenhouse gas emissions reduction and costs savings, c) improving the control of indoor comfort, as well as d) developing innovative control logics or maintenance programs based on

Part of
Pernigotto, G., Ballarini, I., Patuzzi, F., Prada, A., Corrado, V., & Gasparella, A. (Eds.). 2025. Building simulation applications BSA 2024. bu,press.
https://doi.org/10.13124/9788860462022

data-driven automated fault detection and diagnosis methods (Rosato et al., 2022a,b). The BEST Directory of the International Building Performance Simulation Association (IBPSA)-USA website (IBPSA, 2024) lists more than 170 platforms for modelling and simulating building-integrated energy systems; among these software, TRNSYS is recognized in the scientific community as one of the best dynamic simulation tools as it takes into account the intermittent character of loads driven by occupants and the part-load features of generating systems, as well as the interaction between building loads, systems' outputs and climatic data (Sun et al., 2017; Qiu et al., 2020).

However, validation of simulation models is essential to accurately assess the predictive performance with respect to field operation (Granderson et al., 2020). Some scientific studies have faced this issue by developing simulation models of existing HVAC systems (Sun et al., 2017; Montazeri and Kargar, 2020; Kim et al., 2019; Qiu et al., 2020). Sun et al. (2017) developed a simulation model for a single duct dual-fan variable air volume (VAV) AHU installed in a research centre located in Iowa (USA) utilizing the TRSNYS software (TRNSYS, 2024). Montazeri and Kargar (2020) employed the simulation tool HVACSIM+ (HVACSIM+, 2024) to model the same HVAC system operating in USA. On a similar note, Kim et al. (2019) utilized EnergyPlus software (EnergyPlus, 2024) to create a simulation model for an HVAC system including a VAV AHU installed in a small commercial building in Knoxville (USA). Furthermore, TRNSYS has been utilized to simulate a VAV AHU unit installed in a building located in Shanghai (China) by Qiu et al. (2020).

1.2 Novelty, Goals and Structure

In this study, a detailed dynamic simulation model of a single duct constant air volume AHU installed at the SENS-i lab of the Department of Architecture and Industrial Design of the University of Campania Luigi Vanvitelli (south of Italy) has been developed, calibrated, and validated against field experiments performed under various boundary conditions during both summer and winter conditions. Section 2 describes the experimental set-up and tests; Section 3 details the TRNSYS simulation model, while Section 4 illustrates the results of the experimental validation of the proposed model.

The main goals of this study can be summarized as follows: a) make available to stakeholders an experimentally validated digital twin of a typical HVAC system; b) evaluate the capability of TRNSYS platform in modelling a single duct constant air volume AHU; c) assess the model accuracy with respect to Italian climatic conditions covering both summer and winter seasons; d) support a widespread adoption of HVAC systems based on single duct constant air volume AHU for indoor comfort control.

With respect to the scientific studies already available in the literature (Montazeri & Kargar, 2020; Sun et al., 2017; Kim et al., 2019; Qiu et al., 2020), this study is innovative taking into account that a) the aforementioned papers primarily focus on HVAC system operation in the USA or China, overlooking the specific climatic conditions in Italy (it is important to note that climate conditions play a crucial role in the performance of HVAC systems), b) it focuses on a constant air volume AHU, while the other scientific works investigated variable air volume AHUs, and c) only two researchers (Sun et al., 2017; Qiu et al., 2020) utilized the standalone simulation tool TRNSYS in their studies, but only Sun et al. (2017) conducted the experimental validation of the simulation model (to address this gap, the present study integrates both TRNSYS simulation and experimental testing within identical boundary and climate conditions).

2. Experimental Setup and Tests

The SENS i-Lab (SENS i-Lab, 2024), located in the Department of Architecture and Industrial Design of the University of Campania Luigi Vanvitelli (Aversa, southern Italy, latitude: 40°58′21″ North, longitude: 14°12′26″ East), is equipped with a typical HVAC system consisting of a single duct dual-fan constant air volume AHU, able to regulate indoor air temperature, indoor air relative humidity, indoor air velocity and indoor air quality inside a test room. Fig. 1 reports the schematic of the AHU including all the interconnected components: supply air fan (SAF) and return air fan (RAF), humidifier (HUM), cooling coil (CC) coupled with an air-to-water electric refrigerating system (RS) via a cold tank (CT), post-heating coil (PostHC) connected to an air-to-water electric heat pump via a hot tank (HT). A mixture of water and ethylene glycol (6% by volume) is used as a heat carrier fluid. The AHU is fully equipped with accurate sensors to monitor and record all the key operating parameters (shown in Fig. 1). Additional details regarding the AHU components, sensors and control logic strategy can be found in (Rosato et al., 2022a,b).

The experimental electric power $EP_{RAF,EXP}$, $EP_{SAF,EXP}$, $EP_{HUM,EXP}$, $EP_{RS,EXP}$ and $EP_{HP,EXP}$ consumed by the RAF, the SAF, the HUM, the RS, and the HP, respectively, are calculated as follows:

$$EP_{RAF,EXP} = \left(V_{RAF} \cdot A_{RAF}\right)_{EXP} \cdot \cos\varphi_{RAF} \quad \text{Eq. 1}$$

$$EP_{SAF,EXP} = \frac{\left(V_{SAF}^{L1} \cdot A_{SAF}^{L1}\right)_{EXP} \cdot \cos\varphi_{SAF}}{\sqrt{3}} + \frac{\left(V_{SAF}^{L2} \cdot A_{SAF}^{L2}\right)_{EXP} \cdot \cos\varphi_{SAF}}{\sqrt{3}} + \frac{\left(V_{SAF}^{L3} \cdot A_{SAF}^{L3}\right)_{EXP} \cdot \cos\varphi_{SAF}}{\sqrt{3}} \quad \text{Eq. 2}$$

$$EP_{HUM,EXP} = \frac{\left(V_{HUM}^{L1} \cdot A_{HUM}^{L1}\right)_{EXP} \cdot \cos\varphi_{HUM}}{\sqrt{3}} + \frac{\left(V_{HUM}^{L2} \cdot A_{HUM}^{L2}\right)_{EXP} \cdot \cos\varphi_{HUM}}{\sqrt{3}} + \frac{\left(V_{HUM}^{L3} \cdot A_{HUM}^{L3}\right)_{EXP} \cdot \cos\varphi_{HUM}}{\sqrt{3}} \quad \text{Eq. 3}$$

$$EP_{RS,EXP} = \left(V_{RS}^{L1} \cdot A_{RS}^{L1}\right)_{EXP} \cdot \cos\varphi_{RS} + \left(V_{RS}^{L2} \cdot A_{RS}^{L2}\right)_{EXP} \cdot \cos\varphi_{RS} + \left(V_{RS}^{L3} \cdot A_{RS}^{L3}\right)_{EXP} \cdot \cos\varphi_{RS} \quad \text{Eq. 4}$$

$$EP_{HP,EXP} = \left(V_{HP}^{L1} \cdot A_{HP}^{L1}\right)_{EXP} \cdot \cos\varphi_{HP} + \left(V_{HP}^{L2} \cdot A_{HP}^{L2}\right)_{EXP} \cdot \cos\varphi_{HP} + \left(V_{HP}^{L3} \cdot A_{HP}^{L3}\right)_{EXP} \cdot \cos\varphi_{HP} \quad \text{Eq. 5}$$

where $\cos\varphi$ is the power factor (assumed equal to 0.95 as suggested by the manufacturers, whatever the components), A and V represent the electric phase current and phase voltage, respectively, at phase L1 or L2 or L3 measured for each AHU component.

The experimental cooling power $CP_{RS,EXP}$ supplied by the RS, cooling power $CP_{CC,EXP}$ exchanged between air and heat carrier fluid via the CC, thermal power $TP_{HP,EXP}$ supplied by the HP, and thermal energy $TP_{PostHC,EXP}$ exchanged between air and heat carrier fluid via the PostHC are calculated by using the following formulas:

$$CP_{RS,EXP} = \rho_F \cdot c_F \cdot \dot{V}_{F,in,RS,EXP} \cdot \left(T_{F,in,RS,EXP} - T_{F,out,RS,EXP}\right) \quad \text{Eq. 6}$$

$$CP_{CC,EXP} = \rho_F \cdot c_F \cdot \dot{V}_{F,in,CC,EXP} \cdot \left(T_{F,out,CC,EXP} - T_{F,in,CC,EXP}\right) \quad \text{Eq. 7}$$

$$TP_{HP,EXP} = \rho_F \cdot c_F \cdot \dot{V}_{F,in,HP,EXP} \cdot \left(T_{F,out,HP,EXP} - T_{F,in,HP,EXP}\right) \quad \text{Eq. 8}$$

$$TP_{PostHC,EXP} = \rho_F \cdot c_F \cdot \dot{V}_{F,in,PostHC,EXP} \cdot \left(T_{F,in,PostHC,EXP} - T_{F,out,PostHC,EXP}\right) \quad \text{Eq. 9}$$

where $\dot{V}_{F,in,RS,EXP}$, $\dot{V}_{F,in,CC,EXP}$, $\dot{V}_{F,in,HP,EXP}$, and $\dot{V}_{F,in,PostHC,EXP}$ are the measured heat carrier fluid volumetric flowrate entering the RS, the CC, the HP and the PostHC, respectively, $T_{F,in,RS,EXP}$, $T_{F,in,CC,EXP}$, $T_{F,in,HP,EXP}$, and $T_{F,in,PostHC,EXP}$ are the measured temperatures of heat carrier fluid entering the RS, the CC, the HP and the PostHC, respectively, $T_{F,out,RS,EXP}$, $T_{F,out,CC,EXP}$, $T_{F,out,HP,EXP}$, and $T_{F,out,PostHC,EXP}$ are the measured temperatures of heat carrier fluid exiting the RS, the CC, the HP and the PostHC, respectively, ρ_F and c_F are, respectively, the density and the specific heat of heat carrier fluid. The calibration and validation of the developed simulation model were performed by contrasting the predicted values with the data measured during 14 daily experiments, carried out from 9:00 am to 6:00 pm upon varying the boundary climatic conditions during both cooling and heating seasons; in particular, 8 tests were performed during winter (W1, W2, W3, W4, W5, W6, W7, W8), while 6 tests were carried out during summer (S1, S2, S3, S4, S5, S6). In particular, during summer the outdoor air temperature ranged from a minimum of 21.46 °C (test S6) up to a maximum of 41.22 °C (test S3), whereas during winter it varied from a minimum of 6.24 °C (test W5) up to a maximum of 23.85 °C (test W4). Data were measured and recorded every second. Additional details regarding the experimental tests can be found in (Rosato et al., 2024).

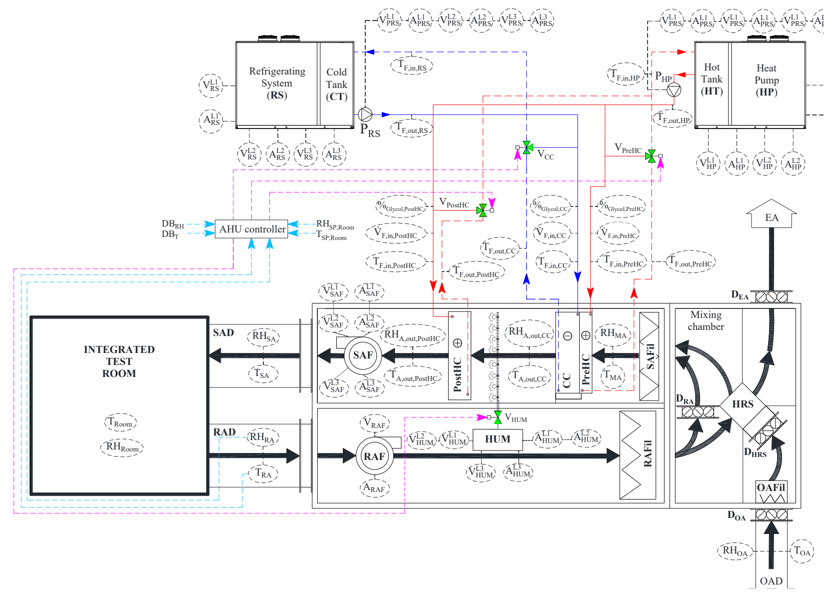

RAD: return air dumper; RAF: return air fan; T_{RA}: return air temperature (°C); RH_{RA}: return air relative humidity (%); SAD: supply air dumper; SAF: supply air fan; T_{SA}: supply air temperature (°C); RH_{SA}: supply air relative humidity (%); HUM: humidifier; RAFil: return air filter; D_{OA}: outdoor air dumper; OAFil: outdoor air filter; T_{OA}: outdoor air temperature (°C); RH_{OA}: outdoor air relative humidity (%); D_{HRS}: heat recovery system dumper; HRS: heat recovery system; D_{RA}: return air dumper; D_{EA}: exhaust air dumper; SAFil: supply air filter; PreHC: pre-heating coil; CC: cooling coil; PostHC: post-heating coil; $T_{F,in,CC}$: heat carrier fluid temperature at cooling coil inlet (°C); $\dot{V}_{F,in,CC}$: volumetric flow rate of cooling coil heat carrier fluid (m³/h); $T_{F,in,PostHC}$: heat carrier fluid temperature at heat pump inlet (°C); $\dot{V}_{F,in,PostHC}$: volumetric flow rate of post-heating coil heat carrier fluid (m³/h); $T_{F,in,RS}$: heat carrier fluid temperature at refrigerating system inlet (°C); $T_{F,in,HP}$: heat carrier fluid temperature at heat pump inlet (°C); HP: heat pump; HT: hot tank; CT: cold tank; RS: refrigerating system.

Fig. 1 – Schematic of the AHU of the SENS i-Lab

3. Simulation Model

In TRNSYS 18 a mathematical model (named "Type") represents each component. Each TRNSYS Type requires some inputs to be specified in order to calculate the corresponding outputs. Fig. 2 presents a flow diagram indicating the main TRNSYS Types used in the model, together with the main corresponding inputs and outputs. In this study, the AHU was simulated with a time-step of 1 second. In the TRNSYS Type 930 (modelling the RAF and the SAF), an energy balance that considers pressure impacts determines the air's output state; the volumetric air flowrate is simulated according to the RAF/SAF velocity set by the end-user electric via specific equations derived from separate experiments. The simulated power consumption $EP_{RAF,SIM}/EP_{SAF,SIM}$ of the RAF/SAF is calculated via the following equations (derived from separate experimental tests) as a function of the RAF/SAF velocity percentage OL_{RAF}/OL_{SAF} (ranging between 0 and 100%) set by the end-user:

$$EP_{RAF,SIM} = -0.000000142 \cdot OL_{RAF}^{\ 5} + 0.00002882 \cdot OL_{RAF}^{\ 4} - 0.0013779 \cdot OL_{RAF}^{\ 3} + 0.040138 \cdot OL_{RAF}^{\ 2} - 0.15187 \cdot OL_{RAF} + 17.101 \qquad \text{Eq.10}$$

$$EP_{SAF,SIM} = 0.0000136 \cdot OL_{SAF}^{\ 4} - 0.0009289 \cdot OL_{SAF}^{\ 3} + 0.14404 \cdot OL_{SAF}^{\ 2} - 1.324 \cdot OL_{SAF} + 87.297 \qquad \text{Eq.11}$$

The mixing of outdoor air and return air is modelled via the TRNSYS Type 648. In the TRNSYS Types 508c and 753e are modelling the CC and the PostHC, respectively; the air is passing over a coil inside which a colder/hotter heat carrier fluid is flowing; these Types use the "bypass fraction approach" to predict the outlet conditions of both heat carrier fluid and air; according to the AHU manufacturer, the bypass fraction is 15% for the CC and 10% for the PostHC. The following equations are used to calculate the simulated cooling power $CP_{CC,SIM}$ and thermal power $TP_{PostHC,SIM}$ supplied by the CC and the PostHC, respectively:

$$CP_{CC,SIM} = \rho_F \cdot c_F \cdot \dot{V}_{F,in,CC,EXP} \cdot \left(T_{F,out,CC,SIM} - T_{F,in,CC,EXP}\right) \qquad \text{Eq.12}$$

$$TP_{PostHC,SIM} = \rho_F \cdot c_F \cdot \dot{V}_{F,in,PostHC,EXP} \cdot T_{F,in,PostHC,EXP} - \rho_F \cdot c_F \cdot \dot{V}_{F,in,PostHC,EXP} \cdot T_{F,out,PostHC,SIM} \qquad \text{Eq.13}$$

where $T_{F,out,CC,SIM}$ and $T_{F,out,PostHC,SIM}$ are the simulated temperature of the heat carrier fluid exiting the CC and the PostHC, respectively.

The TRNSYS Type 941 models a single-stage air-to-water HP/RS. It generates output values for absorbed power, RS cooling capacity, or HP heating capacity. This model requires a performance input map (based on a user-supplied data file) that includes the values of heating capacity and electric power consumption as a function of both outside air temperature and heat carrier fluid temperature entering the HP/RS. The performance maps of the HP and the RS used in this study are reported in Figs. 3 and 4, respectively; they indicate the COefficient of Performance (COP) of the HP (Fig. 3) and the Energy Efficiency Ratio (EER) of the RS (Fig. 4).

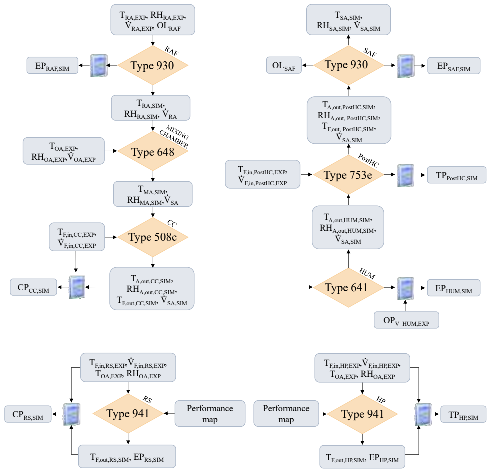

Fig. 2 – Flow chart with inputs and outputs of TRNSYS Types

The values in Figs. 3 and 4 have been obtained by modifying the manufacturer performance maps (derived via the Magellano software developed by the manufacturer itself (AERMEC, 2024)) according to experimental tests conducted in the SENS i-Lab and described in the Section 2. The manufacturer assessed the performance of both the HP and the RS based on experimental tests performed according to (European Standard EN 14825). In particular, with respect to the manufacturer values, both the electric power consumption and the heating power outputs of the HP were decreased by 25%, while the electric power consumption values of the RS were increased by 25% and the cooling power outputs of the RS were reduced by 40% in order to be compliant with the measured values. As a result, the COP values of the HP remained the same as the manufacturer's specifications, while the EER values of the RS decreased by 48% compared to the manufacturer's performance map. The following equations are used in this paper to calculate the simulated values of cooling power $CP_{RS,SIM}$ and thermal power $TP_{HP,SIM}$ supplied by the RS and the HP, respectively:

$$CP_{RS,SIM} = \rho_F \cdot c_F \cdot \dot{V}_{F,in,RS,EXP} \cdot \left(T_{F,in,RS,EXP} - T_{F,out,RS,SIM}\right) \quad \text{Eq.14}$$

$$TP_{HP,SIM} = \rho_F \cdot c_F \cdot \dot{V}_{F,in,HP,EXP} \cdot \left(T_{F,out,HP,SIM} - T_{F,in,HP,EXP}\right) \quad \text{Eq.15}$$

where $T_{F,out,RS,SIM}$ and $T_{F,out,HP,SIM}$ are the simulated temperatures of the heat carrier fluid exiting the RS and the HP, respectively. In the TRNSYS Type 641 (modelling the humidifier), the outlet state of the air is defined based on an energy balance where the heat losses are neglected. The following equation is derived from measured data to calculate the simulated humidifier electric power consumption $EP_{HUM,SIM}$ as a function of the measured opening percentage $OP_{V,HUM,EXP}$ (ranging between 0 and 100%) of the valve supplying the humidifier:

$$EP_{HUM,SIM} = OP_{V,HUM,EXP} \cdot 34.022 \quad \text{Eq.16}$$

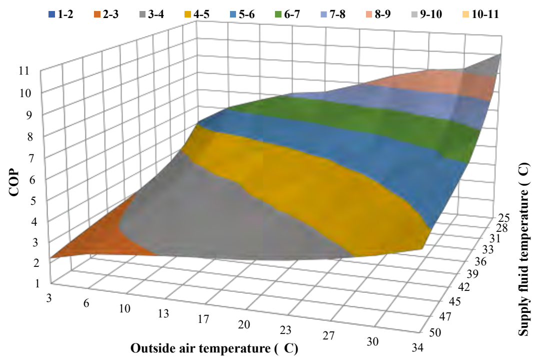

Fig. 3 – COP of the HP upon varying T_{OA} and $T_{F,out,HP}$

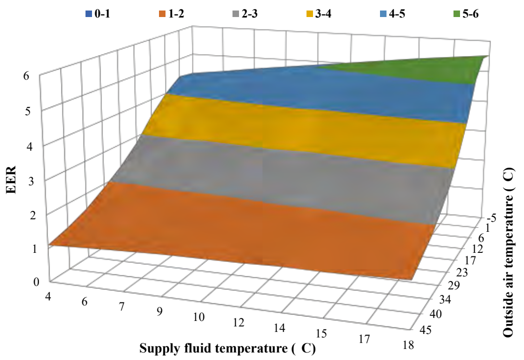

Fig. 4 – EER of the RS upon varying T_{OA} and $T_{F,out,RS}$

4. Experimental Validation of the Simulation model

The proposed TRNSYS model has been validated by comparing the simulation results with 453,600 experimental data points. The Eq. 17 is used to calculate the percentage difference between the simulated and experimental daily values of electric (EE), cooling (CE), and thermal energy (TE) for each component of the AHU, including SAF, RAF, HUM, RS, HP, CC, and PostHC:

$$\Delta X_Y = \frac{\left(X_{Y,SIM} - X_{Y,EXP}\right)}{X_{Y,EXP}} \cdot 100 \quad \text{Eq.17}$$

where $X_{Y,SIM}$ is the simulation value of EE/CE/TE associated to the specific AHU component Y, while $X_{Y,EXP}$ is the experimental value of EE/CE/TE associated to the same AHU component Y obtained during the same test. Figs. 5 and 6 report the values of ΔEE_{SAF}, ΔEE_{RAF}, ΔEE_{HUM}, ΔEE_{RS}, ΔEE_{HP}, ΔCE_{RS}, ΔCE_{CC}, ΔTE_{HP} and ΔTE_{PostHC} as a function of the summer and winter tests, respectively. In this context, positive values indicate that the simulated energy values are greater than the measured values. Tables 1 and 2 indicate the minimum and maximum values of the parameters ΔEE_{SAF}, ΔEE_{RAF}, ΔEE_{HUM}, ΔEE_{RS}, ΔEE_{HP}, ΔCE_{RS}, ΔCE_{CC}, ΔTE_{HP} and ΔTE_{PostHC} during summer and winter, respectively, also indicating the test corresponding to the minimum/maximum value. The results illustrate that the proposed model effectively captures the real-world performance of both the SAF and the RAF. This is evident from the values of ΔEE_{SAF} and ΔEE_{RAF}, consistently ranging from -3.4% to 3.8% for each respective field. The variations in percentages observed between the experimental and simulated values can be attributed to the utilization of equations derived from interpolated experimental electric demands to calculate the electric energy consumption of the simulated SAF and RAF; while these equations exhibit high R^2 values exceeding 0.99, they do not entirely capture the transient behaviour of the SAF and RAF, particularly during the initial stages of testing. The comparison of measured and predicted values highlights the overall accuracy of the simulation for both the RS and HP systems, although there is room for improvement, as indicated by the largest deviations observed: -15.3% for ΔEE_{RS}, -9.9% for ΔCE_{RS}, -10.6% for ΔEE_{HP}, and -10.5% for ΔTE_{HP}. These percentage differences can be explained by taking into account that the TRNSYS Type 941 does not consider the transient effects of both the inlet fluid temperature and the outdoor air temperature, but it assumes a steady-state operation of both the RS and the HP (while a transient behaviour is usually recognized during field tests). With respect to the humidifier, it can be noticed that the parameter ΔEE_{HUM} is characterized by a minimum value of -9.1% (test W3) during winter, while its maximum value is 4.2% during summer. The differences between the experimental and simulated data can be attributed to the fact the HUM electric energy consumption has been evaluated based on an equation interpolating the measured values and, therefore, it is not always able to accurately capture the transient operation of the HUM, especially at the beginning of its activation requiring a few minutes to reach steady-state conditions.

Table 1 – Minimum and maximum values of ΔEE_{SAF}, ΔEE_{RAF}, ΔEE_{HUM}, ΔEE_{RS}, ΔEE_{HP}, ΔCE_{RS}, ΔCE_{CC}, ΔTE_{HP} and ΔTE_{PostHC} with reference to the summer tests

	Minimum	**Maximum**
ΔEE_{SAF}	1.4% (test S5)	3.8% (test S2)
ΔEE_{RAF}	-1.8% (test S1)	0.2% (test S4)
ΔEE_{HUM}	-5.4% (test S4)	4.2% (test S1)
ΔEE_{RS}	1.9% (test S4)	8.4% (test S6)
ΔEE_{HP}	-10.6% (test S6)	3.4% (test S5)
ΔCE_{RS}	-9.9% (test S3)	3.8% (test S1)
ΔCE_{CC}	-3.9% (test S4)	1.1% (test S6)
ΔTE_{HP}	-8.3% (test S6)	1.6% (test S3)
ΔTE_{PostHC}	0.0% (test S6)	4.85% (test S3)

Table 2 – Minimum and maximum values of ΔEE_{SAF}, ΔEE_{RAF}, ΔEE_{HUM}, ΔEE_{RS}, ΔEE_{HP}, ΔCE_{RS}, ΔCE_{CC}, ΔTE_{HP} and ΔTE_{PostHC} with reference to the winter tests

	Minimum	**Maximum**
ΔEE_{SAF}	-2.4% (test W7)	2.1% (test W1)
ΔEE_{RAF}	-3.4% (test W5)	-2.4% (test W1)
ΔEE_{HUM}	-9.1% (test W3)	-2.4 % (test W2)
ΔEE_{RS}	-15.3% (test W1)	4.9% (test W4)
ΔEE_{HP}	-9.8% (test W7)	9.7% (test W4)
ΔCE_{RS}	-8.6% (test W7)	1.6% (test W2)
ΔCE_{CC}	-5.7% (test W6)	18.3% (test W1)
ΔTE_{HP}	-10.5% (test W7)	3.9% (test W2)
ΔTE_{PostHC}	-6.0% (test W3)	-1.9% (test W1)

In particular, during the W3 test the humidifier was activated only 4 times, each time for a limited period of about 7 minutes, with significant unsteady operation. In relation to the CC and the PostHC, the variance between simulated and measured performance (with the highest deviations being 18.3% and -6.0%, respectively) can be ascribed to two primary factors: a) air temperature is measured in a single specific point (while a non-uniform air temperature distribution is generally recognized at the inlet and outlet), and b) a constant bypass factor is assumed (even if it changes with the operating conditions).

5. Conclusion

In this paper, a detailed dynamic simulation model of a typical HVAC system including a single duct dual-fan constant air volume air-handling unit has been developed and experimentally validated via the software TRNSYS 18. The comparison between simulation and measured data underlined a high degree of accuracy of the model in reflecting the measured field performance, with maximum percentage differences between predicted and experimental values up to -6.0%, 18.3%, -9.1%, -10.6%, -15.3% in terms of heating coil energy, cooling coil energy, humidifier electric demand, heat pump electric consumption and refrigerating system electricity request, respectively. Therefore, the analysis highlighted a) the capability of TRNSYS platform in simulating complex system dynamics and its utility in advancing HVAC research and design, as well as b) the accuracy and efficacy of the developed simulation model in capturing real-world performance of the HVAC system. However, there are still shortcomings due to its inability to fully represent and simulate the transient operation of AHU components (and this is one of the main reasons causing the discrepancies between predicted and measured data). Future work will focus on enhancing the accuracy of the proposed AHU digital twin, with particular reference to the heat pump and the refrigerating system, by means of artificial neural network-based models (trained based on the field performance values) allowing to accurately represent the system beyond its steady-state functioning.

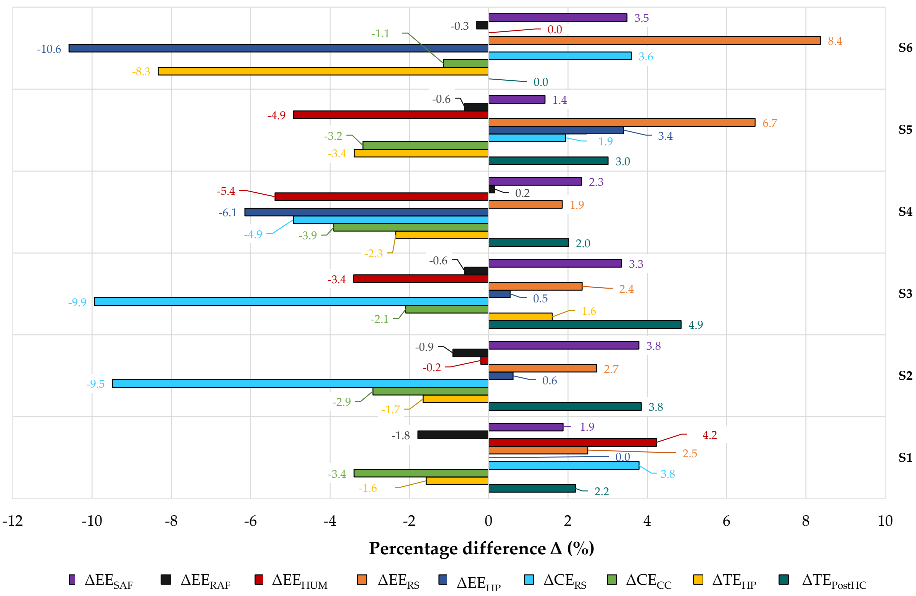

Fig. 5 – Percentage difference between simulated and experimental performance of AHU components as a function of summer tests

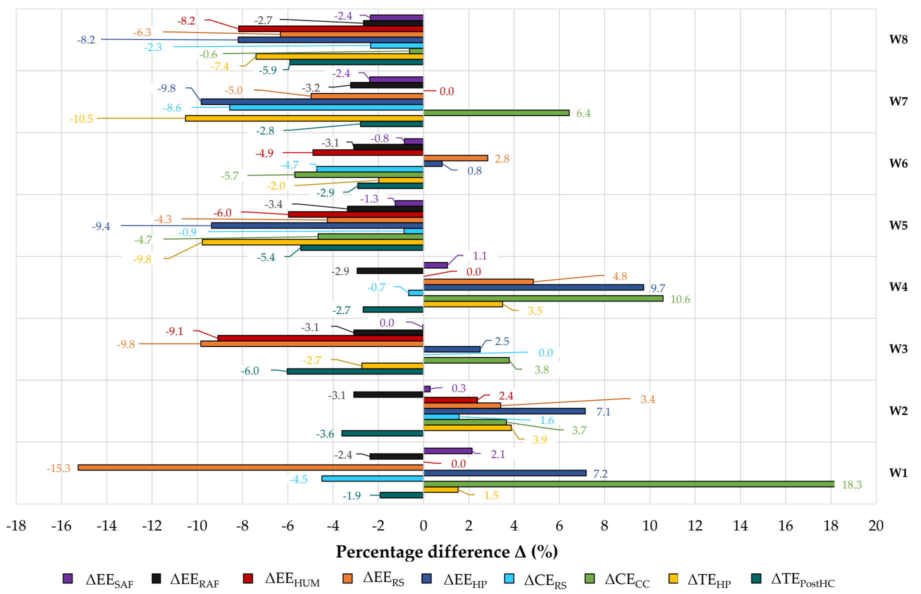

Fig. 6 – Percentage difference between simulated and experimental performance of AHU components as a function of winter tests

Acknowledgement

This study has been performed within the activities of the research project titled "UTMOST FDD: an aUToMated, Open, Scalable and Transparent Fault Detection and Diagnosis process for air-handling units based on a hybrid expert and artificial intelligence approach. From experimental open data to transfer model learning for the enhancement of energy management and indoor environmental quality in buildings" funded by the call "PRIN 22" (CUP: E53D23002840006).

Nomenclature

Symbols

A	Current intensity (A)
AHU	Air-handling unit
CC	Cooling coil
CE	Cooling energy (kWh)
COP	Coefficient of performance
CP	Cooling power (kW)
D	Percentage difference (%)
EE	Electric energy (kWh)
EER	Energy efficiency ratio
EP	Electric power (W)
HP	Heat pump
HUM	Humidifier
HVAC	Heating, ventilation and air-conditioning
OL	Velocity percentage (%)
OP	Opening percentage (%)
PostHC	Post-heating coil
RAF	Return air fan
RS	Refrigerating system
S1-S6	Tests performed during summer
SAF	Supply air fan
T	Temperature (°C)
TE	Thermal energy (kWh)
TP	Thermal power (kW)
V	Voltage (V)
$\dot{V}$	Volumetric flow rate (m³/s)
VAV	Variable air volume
W1-W8	Tests performed during winter

Subscripts

CC	Cooling coil
EXP	Experimental
F	Heat carrier fluid
HP	Heat pump
HUM	Humidifier
PostHC	Post-heating coil
RAF	Return air fan
RS	Refrigerating system
SAF	Supply air fan
SIM	Simulated data

References

AERMEC. https://global.aermec.com/en/download/product-selection/

Cao, X., X. Dai, and J. Liu. 2016. "Building energy-consumption status worldwide and the state-of-the-art technologies for zero-energy buildings during the past decade". *Energy and buildings* 128: 198-213. https://doi.org/ 10.1016/j.enbuild.2016.06.089

EnergyPlus. https://energyplus.net/

European Standard EN 14825: Air conditioners, liquid chilling packages and heat pumps, with electrically driven compressors, for space heating and cooling – Testing and rating at part load conditions and calculation of seasonal performance (2022)

Global Status Report for Buildings and Construction. Towards a Zero-Emission, Efficient and Resilient Buildings and Construction Sector. Available online: https://www.unep.org/resources/publication/2022-global status-report-buildings-and-construction

Granderson, J., G. Lin, A. Harding, P. Im and Y. Chen. 2020. "Building fault detection data to aid diagnostic algorithm creation and performance testing". *Scientific data. 7*(1): 65. https://doi.org/ 10.6084/m9.Fig.share.11743074

HVACSIM+. Available online: https://www.nist.gov/services-resources/software/hvac-simulation-plus-other-systems-hvacsim

Kim, J., S. Frank, J. E. Braun and D. Goldwasser. 2019. "Representing small commercial building faults in energyplus, Part I: Model development". *Buildings* *9*(11): 233. https://doi.org/ 10.3390/buildings9110233

Mirnaghi, M. S., and F. Haghighat. 2020. "Fault detection and diagnosis of large-scale HVAC systems in buildings using data-driven methods: A comprehensive review"- *Energy and Buildings* 229: 110492. https://doi.org/ 10.1016/j.enbuild.2020.110492

Mitali, R., S. Padarbinda, and C. K. Panigrahi. 2023. "The influencing factors on efficacy enhancement of HVAC systems. A review". *Materials Today: Proceedings* 80: 3423-3432. https://doi.org/ 10.1016/j.matpr.2021.07.264

Montazeri, A., and S. M. Kargar. 2020. "Fault detection and diagnosis in air handling using data-driven methods". *Journal of Building Engineering* 31: 101388. https://doi.org/ 10.1016/j.jobe.2020.101388

Qiu, A., Z. Yan, Q. Deng, J. Liu, L. Shang, and J. Wu. 2020. "Modeling of HVAC systems for fault diagnosis". *IEEE Access* 8: 146248-146262. https://doi.org/ 10.1109/ACCESS.2020.3015526

Rosato, A., F. Guarino, M. El Youssef, A. Capozzoli, M. Masullo, and L. Maffei. 2022a. "Experimental assessment of ground-truth faults in a typical single-duct dual-fan air-handling unit under Mediterranean climatic conditions: Impact scenarios of sensors' offset and fans' failure". *Energy and Buildings* 275. https://doi.org/ 10.1016/j.enbuild.2022.112492

Rosato, A., F. Guarino, M. El Youssef, A. Capozzoli, M. Masullo, and L. Maffei. 2022b. "Faulty Operation of Coils' and Humidifier Valves in a Typical Air-Handling Unit: Experimental Impact Assessment of Indoor Comfort and Patterns of Operating Parameters under Mediterranean Climatic Conditions". *Energies* 15(18). https://doi.org/ 10.3390/en15186781

Rosato, A., R. Mercuri, M. Bashir, H. Daoud, and M. El Youssef. 2024. "14 kW Air-To-Water Vapor-Compression Electric Heat Pump and Refrigerating System Operating in Southern Italy: Field vs. Rated Performance". *Smart Innovation, Systems and Technologies* 378. https://doi.org/ 10.1007/978-981-99-8501-2_52

SENS i-Lab, Department of Architecture and Industrial Design, University of Campania Luigi Vanvitelli, https://www.architettura.unicampania.it/images/ricerca/laboratori/EN/SENS-i_Lab_2021_EN.pdf

Sun J., G. Hu, and C. J. Spanos. *2017*. "Development and verification of a multizone building HVAC model with TRNSYS." *12th IEEE Conference on Industrial Electronics and Applications (ICIEA)* 887-894. https://doi.org/ 10.1109/ICIEA.2017.8282965

TRNSYS 18. https://www.trnsys.com/.